Improved Strategy in Analytic Surface Calculation for Molecular Systems: Handling of Singularities and Computational Efficiency

Frank Eisenhaber* and Patrick Argos

European Molecular Biology Laboratory, D-69012 Heidelberg, Germany

Received 12 November 1992; accepted 26 May 1993

Computer methods for analytic surface calculations of molecular systems suffer from numerical instabilities and are CPU time consuming. In this article, we present proposals toward the solution of both problems. Singularities arise when nearly collinear triples of neighboring atoms or multiple vertices are encountered during the calculation. Topological decisions in analytic surface calculation algorithms (accessibility of vertices and arcs) are based upon the comparison of distances or angles. If two such numbers are nearly equal, then currently used computer programs may not resolve this ambiguity correctly and can subsequently fail. In this article, modifications in the analytic surface calculation algorithm are described that recognize singularities automatically and treat them appropriately without restarting parts of the computation. The computing time required to execute these alterations is minimal. The basic modification consists in defining an accuracy limit within which two values may be assumed as equal. The search algorithm has been reformulated to reduce the computational effort. A new set of formulas makes it possible to avoid mostly the extraction of square roots. Tests for small- and medium-sized intersection circles and for pairs of vertices with small vertex height help recognize fully buried circles and vertex pairs at an early stage. The new program can compute the complete topology of the surface and accessible surface area of the protein crambin in 1.50–4.29 s (on a single R3000 processor of an SGI 4D/480) depending on the compactness of the conformation where the limits correspond to the fully extended or fully folded chain, respectively. The algorithm, implemented in a computer program, will be made available on request.

INTRODUCTION

Solvent interactions are thought to be among the most important molecular forces that guide biomacromolecules to their folded forms in the native environment.[1–4] The free energy of a system of a solute molecule embedded in a solvent consists of the dispersion effect, the cavity (excluded volume) contribution, and, for polar molecules, also of the electrostatic component.[5,6] Experimental data confirm that the solvation energy, especially its dispersion and cavity portions, is proportional to the surface area of exposed atomic groups of the solute.[7–11] In the assumption of additivity of atomic contributions, the surface area-based component of the solvation energy is assumed equal to the sum of products of the solvent-accessible (or molecular) surface area attributed to a certain atom and an energy factor specific for a given type of atom.[12,13]

The solvent-accessible surface[14] is that part of the surface of a sphere centered at an atom and with radius $r_{vdW} + r_{sol}$, where the center of a spherical solvent molecule (r_{sol}) can be placed in contact with the atomic van der Waals sphere (r_{vdW}) without penetrating other atoms. The molecular surface[15] is the envelope of the molecular volume from which solvent is excluded. The accurate methods for calculating molecular surfaces can be grouped into numerical[14,16–20] and analytic[21–25] integration approaches. The latter are attractive for molecular mechanics calculations because (1) the accuracy of the calculations is only limited by the floating-point arithmetics of the computer used, (2) the molecular surface and the accessible surface can be immediately obtained from the same set of accessible vertices and arcs, and (3) the derivatives of the surface elements with respect to the atomic coordinates (Cartesian[23,26] or internal[27]) are available in analytic form. However, the application scope of analytic surface calculation methods is limited because (1) the algorithms show numerical instabilities if multiple vertices and collinear atoms occur and (2) they are CPU time demanding. We present proposals toward a solution of both problems.

Topological decisions (accessibility of surface elements) are based upon the comparison of distances and angles that are calculated only with finite accuracy on computers. For example, a vertex is de-

*Author to whom all correspondence should be addressed.

CCC 0192-8651/93/111272-09

fined as an intersection point of three spheres. The vertex may be buried by one of the mutual neighbors of the atoms i, j, and k. This is the case if the distance between the vertex and a neighboring atom l is less than $r_{vdW}^{(l)} + r_{sol}$. If it is larger for all neighbors, the vertex is declared as accessible. The case of equality that results in a vertex with more than three arcs as well as the problem of inaccurate computation has not been considered. In such ambiguous cases, the algorithm may fail. The consequences are discussed in detail by Perrot et al. (see pp. 5 and 10 of ref. 26). Therefore, the error is not of a numerical nature as usually encountered in numerical methods (question of grid fineness[14,16–20]). The error is a topological one, and the area inaccuracy may be large depending on wrongly described surface fraction.

When singularities occur, Perrot et al.[26] advise modifying a few atom coordinates by ±0.1 Å prior to a restart. In his program "PQMS," Connolly[28] proposed if four spheres intersect in one point to remove the singularity by increasing successively the atomic radii. However, the latter technique fails in symmetric cases. Small changes in parameters such as atom radii and coordinates are not directly linked with the occurrence of the singularity but represent subjective interventions and are also nonpractical if many conformations were to be analyzed. In this article, we describe modifications that can be directly incorporated into analytic surface calculation algorithms such that singularities are automatically recognized and properly treated without restarts. The basic change consists in defining an accuracy limit within which two distances or angles may be assumed as equal.

The most time-consuming part of analytic surface calculations is the determination of the accessibility of vertices and intersection circles. The vast majority do not contribute to the surface. For example, in flavodoxin (3FXN) about 90% of all intersection circles and vertices are completely buried. We reformulate the search algorithm in such a manner that many buried intersection circles are recognized at an early stage and, consequently, a large number of vertices need not be considered at all. Further, in our new set of formulas the extraction of square roots is avoided when possible. We also describe an effective strategy for cycle formation. Together, the improvements reduce the CPU time consumption to that of effective numerical integration procedures.

CALCULATION METHODS

Among the three formal analytic approaches to calculate the surface in a set of interpenetrating spheres (Connolly,[21,22] Richmond,[23] Gibson and Scheraga[24,25]), Connolly's vector formulation is the most straightforward and yet complete. The solution of Perrot et al.[26] is suitable where (1) only one molecule is present, (2) free circles are absent, and (3) internal cavities do not exist. We rely on the results of Connolly.[21,22]

The following notation is used: $\mathbf{a}_i$, $\mathbf{a}_j$, $\mathbf{a}_k$, ... for the coordinates of atoms $i, j, k, \ldots$; r_i, r_j, r_k, ... for the sums of the van der Waals and solvent radii for each respective atom (subsequently referred to as the atomic radius); d_{ij} for the distance between atoms i and j; r_{ij} and $\mathbf{t}_{ij}$, respectively, for the radius and the center of the intersection circle resulting from two overlapping atomic spheres i and j; $\mathbf{p}_{ijk}$ for the vertex (intersection point) of spheres i, j, and k; and $\mathbf{b}_{ijk}$ for the base point of the perpendicular from $\mathbf{p}_{ijk}$ onto the plane defined by atoms i, j, and k (see Fig. 1).

Recognition and Handling of Singularities

The identity of two points $\mathbf{p}_1$ and $\mathbf{p}_2$ of the accessible surface is assumed if their distance $|\mathbf{p}_1 - \mathbf{p}_2|$ is less than a user-defined value ε in an effort to avoid short arc lengths, too near vertices, too small intersection circles, and the like. The value ε should be chosen such that the machine-defined accuracy of real values obtained during the computations for comparison is certainly better than ε. As a result, two values that should be equal by theoretical considerations are recognized as such by the algorithm.

Topological decisions based on the comparison of floating-point numbers are to be taken at the following steps[21]:

1. neighbor relationship of atoms i and j;
2. collinearity of three mutually neighboring atoms i, j, k;
3. existence of common vertices $\mathbf{p}_{ijk}$ of atoms i, j, and k; and
4. tests for collision of $\mathbf{p}_{ijk}$ with other atoms and handling of the case when $\mathbf{p}_{ijk}$ is on the surface of other atoms.

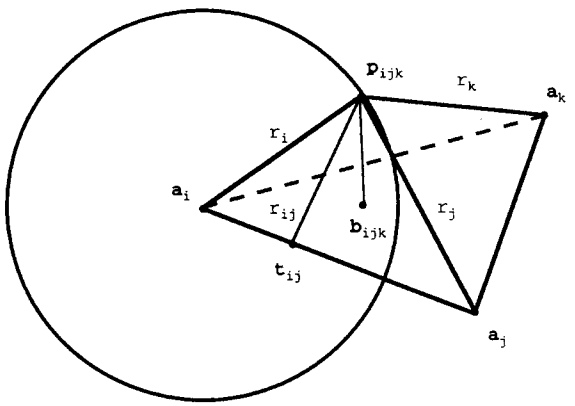

Figure 1. Illustration of the notations used for vectors, points, and distances. The vertex height h_{ijk} is the distance between the vertex point $\mathbf{p}_{ijk}$ and the base point $\mathbf{b}_{ijk}$ of the perpendicular from $\mathbf{p}_{ijk}$ onto the plane defined by atoms i, j, and k.

Neighbor Relationship of Atoms i and j

Two atoms are considered neighboring if the common region of these two spheres is larger than a sphere with radius ε and none of the two spheres fully occludes the other. Five cases encompassing the possible spatial relationships between two spheres i and j can be distinguished:

$$r_i + r_j \leq d_{ij} - \varepsilon \quad (1)$$

$$d_{ij} \geq r_i + r_j > d_{ij} - \varepsilon \quad (2)$$

$$r_i + r_j > d_{ij} > |r_i - r_j| \quad (3)$$

$$d_{ij} \leq |r_i - r_j| < d_{ij} + \varepsilon \quad (4)$$

and

$$d_{ij} + \varepsilon \leq |r_i - r_j| \quad (5)$$

For (1), the two spheres have no point in common while under condition (5) one sphere fully includes the other. Conditions (2) and (4) describe touching spheres. In the third case, the radius of an intersection circle can be calculated as

$$r_{ij} = \frac{1}{2d_{ij}} \sqrt{[(r_i + r_j)^2 - d_{ij}^2][d_{ij}^2 - (r_i - r_j)^2]}$$

If $r_{ij} < \varepsilon$, the two spheres touch each other. Only if $r_{ij} \geq \varepsilon$ are the two atoms i and j recognized as neighbors. The relative error in the surface area determination of sphere i, if atom j was wrongly excluded from the neighbor list, is in the range of

$$\frac{2\pi r_i(r_i - \sqrt{r_i^2 - \varepsilon^2})}{4\pi r_i^2} \approx \frac{1}{4} \cdot \frac{\varepsilon^2}{r_i^2}$$

For faster computation, it is adequate for most cases to test sufficient inequalities. For example, if

$$(r_i + r_j)^2 + [4\varepsilon \cdot \max_i(r_i) + \varepsilon^2] \leq d_{ij}^2$$

then the two spheres i and j are certainly not neighbors nor do they touch each other. If

$$(r_i + r_j)^2 + [2\varepsilon^2 - 4\sqrt{2\varepsilon} \cdot \max_i(r_i)] \geq d_{ij}^2$$

and

$$(r_i - r_j)^2 + [2\varepsilon^2 + 4\sqrt{2\varepsilon} \cdot \max_i(r_i)] \leq d_{ij}^2$$

then the two atoms are certainly neighbors. The constant terms are computed only once. The more delicate cases can also be investigated without the extraction of square roots by checking subsequently the following inequalities:

$$A_1 \leq -2\varepsilon(r_i + r_j) - \varepsilon^2, A_1 \leq 0,$$

$$A_2 \leq 0, \quad \text{and} \quad \frac{A_1 \cdot A_2}{4d_{ij}} \geq \varepsilon^2$$

Here, A_1 and A_2 denote $(r_i + r_j)^2 - d_{ij}^2$ and $d_{ij}^2 - (r_i - r_j)^2$.

Collinearity of Neighboring Atoms i, j, and k

The angle between the vectors $\mathbf{a}_j - \mathbf{a}_i$ and $\mathbf{a}_k - \mathbf{a}_i$ is calculated to obtain the plane normal. The three atoms are considered collinear if the smallest angle in the triangle has a sine near zero (Fig. 1). A measure ε_a for this sine being small can be derived from ε. We use the maximal radius as a scaling factor:

$$\varepsilon_a = \frac{\varepsilon}{\max_i(r_i)}$$

We check the condition that

$$\frac{2 \cdot (d_{ij}^2 \cdot d_{ik}^2 + d_{ij}^2 \cdot d_{jk}^2 + d_{ik}^2 \cdot d_{jk}^2) - d_{ij}^4 - d_{ik}^4 - d_{jk}^4}{d_{ij}^2 \cdot d_{ik}^2} \geq \varepsilon_a^2$$

where d_{ij} and d_{ik} are the two longer edges. The numerator of the last expression is 16 times the squared area of the triangle (i,j,k). In the case of collinearity, one or two of the three circles, ij, ik, and jk are not accessible. The intersection circle ij is buried by atom k if

$$(r_k - \varepsilon)^2 \geq r_{ij}^2 + |\mathbf{t}_{ij} - \mathbf{a}_k|^2$$

If none of the three intersection circles are recognized as buried, then all three are assumed as identical. Then, the two intersections involving the smallest atom are flagged as buried.

Existence of Common Vertices $\mathbf{p}_{ijk}$ of Atoms i, j, and k

The expression

$$A = \frac{A_1 + A_2 + A_3 - d_{ij}^2 d_{ik}^2 d_{jk}^2}{2 \cdot (d_{ij}^2 \cdot d_{ik}^2 + d_{ij}^2 \cdot d_{jk}^2 + d_{ik}^2 \cdot d_{jk}^2) - d_{ij}^4 - d_{ik}^4 - d_{jk}^4}$$

where

$$A_1 = (d_{ij}^2 + d_{ik}^2 - d_{jk}^2) \cdot (r_i^2 d_{jk}^2 + r_j^2 r_k^2)$$

$$A_2 = (d_{ij}^2 - d_{ik}^2 + d_{jk}^2) \cdot (r_j^2 d_{ik}^2 + r_i^2 r_k^2)$$

and

$$A_3 = (-d_{ij}^2 + d_{ik}^2 + d_{jk}^2) \cdot (r_k^2 d_{ij}^2 + r_i^2 r_j^2)$$

determines the square of the orthogonal distance h_{ijk} of the vertex $\mathbf{p}_{ijk}$ from the plane ijk (Fig. 1). The value A may be equal to zero within the accuracy limit ε^2. In such a case, the three intersection circles ij, ik, and jk are considered as touching at the point $\mathbf{b}_{ijk}$. Any one of the three circles may touch the corresponding third atom from within. This intersection circle is not accessible, i.e., if

$$|\mathbf{t}_{ij} - \mathbf{a}_k|^2 + r_{ij}^2 < r_k^2$$

then atom k buries circle ij. The error in the atomic surface area caused by declaring a small but positive value A as indistinguishable from zero can be cal-

culated with the Gauss–Bonnet formula[29] and it is in the same range as in the case of wrongly rejected atoms from the neighbor list (see the section on neighbor relationship).

If the value $A \leq -\varepsilon^2$, then one of the intersection circles must be buried. The circle can be identified as in the previous case.

Tests for Collision of $\mathbf{p}_{ijk}$ with Other Atoms and Handling of the Case when $\mathbf{p}_{ijk}$ Is on Their Surface

For the case $A \geq \varepsilon^2$, two intersection points of the spheres i, j, and k exist. Each of the vertices $\mathbf{p}_{ijk}$ may be buried by a fourth atom l. It is sufficient to examine only the atoms $l_1, l_2, \ldots, l_N$ that are neighbors of i, j, and k or that at least touch these atoms. If an atom l exists such that

$$|\mathbf{a}_l - \mathbf{p}_{ijk}|^2 \leq (r_l - \varepsilon)^2$$

then the vertex $\mathbf{p}_{ijk}$ is certainly buried by atom 1. The vertex is outside of the sphere 1 in the case of

$$|\mathbf{a}_l - \mathbf{p}_{ijk}|^2 \geq (r_l + \varepsilon)^2$$

Otherwise, the vertex is assigned a reserved status with two options. It is assumed to be on the surface of atom 1 with the possibility to be fully buried if

$$|\mathbf{a}_l - \mathbf{p}_{ijk}|^2 \leq r_l^2$$

Otherwise, the vertex is considered to be on the surface of atom 1 with the possibility to be fully accessible. The topological closure of cycles[21] allows to decide at a later stage whether the reserved vertex is really on the surface.

Let us consider a vertex $\mathbf{p}_{ijk}$ that is not buried by any of the atoms of the molecule and is located on the surface of spheres $m_1, m_2, \ldots, m_M$ ($i, j, k \neq m_n$, $n = 1, 2, \ldots, M$). We must now investigate whether the circular arcs ij, ik, and jk leaving $\mathbf{p}_{ijk}$ in the direction of $\mathbf{p}_{ijk} - \mathbf{b}_{ijk}$ continue inside or outside of the spheres m (Fig. 2). For the circle ij, this is performed by comparing the angle α_m between the vectors $\mathbf{p}_{ijk} - \mathbf{a}_m$ and $(\mathbf{t}_{ij} - \mathbf{a}_i) \times (\mathbf{p}_{ijk} - \mathbf{t}_{ij})$ with $\pi/2$ (Fig. 1). The latter is the tangent vector of circle ij in point $\mathbf{p}_{ijk}$. If α_m is in the interval $[0, (\pi/2) - \varepsilon_a]$, then the arc is considered as accessible. The arc ij continues interior to sphere m if α_m is in the interval $[(\pi/2) + \varepsilon_a, \pi]$. In the remaining cases, the circular arc ij is considered to be on the surface of sphere m in some environment of point $\mathbf{p}_{ijk}$, i.e., the circle ij touches the sphere m. Consequently, the intersection circle ij will be: (1) on the surface of sphere m if the atoms i, j, and m are collinear (see the section on collinearity); (2) fully interior to sphere m and touching it at point $\mathbf{p}_{ijk}$ if

$$|\mathbf{t}_{ij} - \mathbf{a}_m|^2 + r_{ij}^2 < r_m^2$$

or (3) fully exterior to sphere m and touching it at $\mathbf{p}_{ijk}$.

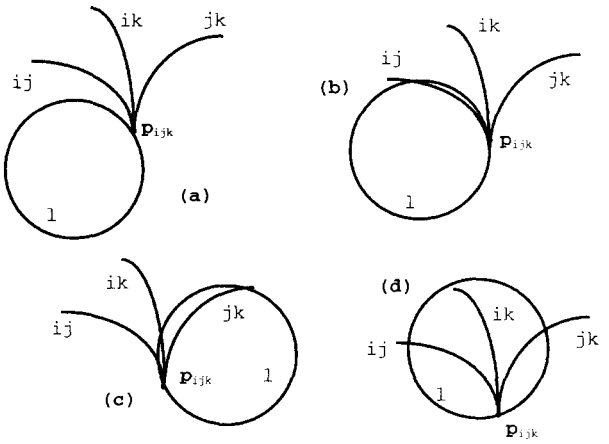

Figure 2. A vertex $\mathbf{p}_{ijk}$ on the surface of a fourth sphere. This schematic drawing illustrates the possible relationships between the three arcs leaving the vertex $\mathbf{p}_{ijk}$ in the direction $\mathbf{p}_{ijk} - \mathbf{b}_{ijk}$ and the fourth sphere l of which a circular cross section is shown. Zero (a), one (b), two (c), or three (d) arcs may be buried in some environment of the vertex $\mathbf{p}_{ijk}$ by the atom 1. In the latter two cases, the vertex is recognized as not accessible. In the former two, the vertex is assumed to be on the accessible surface. If only two arcs of the vertex are not buried, the vertex has specific properties (see the fourth section of the calculation method section).

As a result of the preceeding analysis, 0, 1, 2, or 3 arcs at $\mathbf{p}_{ijk}$ (parts of the intersection circles ij, ik, jk) may be marked as accessible in some environment of the vertex $\mathbf{p}_{ijk}$ (Fig. 2) for the surface case option of the vertex. If this vertex has also the possibility to be accessible, then arcs accessible in the surface case are accessible in any case. If the vertex has the possibility to be buried, then the arcs buried in the surface case are buried under any conditions. The status of the remaining arcs in the vicinity of the vertex under consideration is unclear and must be determined later through the topological closure of cycles and multiple vertices.

If no or only one arc is accessible, then the vertex is defined as buried. If three arcs are exposed, then the vertex is treated classically.[21] If only two arcs are marked as accessible, then this vertex has specific properties. If the arcs of the intersection circles ij and ik are flagged as not buried, then the vertex $\mathbf{p}_{ijk}$ is considered a part of the surface boundary of atom i and only of this atom, whereas a normal vertex is a part of the surface boundary of all three atoms i, j, and k. Several such particular vertices form a multiple vertex.

The determination of the cycles may lead to several variants of complete topological closure on a given atom taking into account both the buried and accessible states of unclear arcs. In any case, we reject cycles with consecutive vertices having a distance less than ε. Then, we check the consistency of the pattern of buried and accessible arcs of vertices with reserved status. An unclear arc buried on

one atom must be buried also on the neighboring atom. As a rule, already at this stage only one variant is left. Further selection criteria include the minimal number of vertices with buried unclear arcs and the minimal number of multiple vertices. Theoretically, it can happen that a complete cycle is formed only from unclear arcs. For this atom, we calculate numerically its accessible surface and select the variant with the nearest area value.

Enhancing Computational Efficiency

The analytic surface calculation involves three principal steps: (1) formation of the neighbor list; (2) determination of the list of fully or partly accessible intersection circles and vertices; and (3) closure of cycles and the area calculation.

The CPU time for step 1 can be decreased by introducing classes of atoms (in one residue or in one space cube) and then checking only the distance to the class center while taking into account the class dimensions.[26,30,31] Normally, residue descriptions are supplied together with the coordinates (e.g., PDB format[32]). We group the atoms in residues.

Part 2 was improved through the following elements: the assignment of states to intersection circles, two fast tests as sufficient criteria to complete nonaccessibility for small- and medium-sized intersection circles, a test to check whether two symmetric vertices with small vertex height are buried, and a search procedure almost without the extraction of square roots. The fast tests are based on the statistics of circle radii and vertex heights in globular proteins.

The accessibility status of an intersection circle can have six different integral values:

$$\text{FREE} < \text{NUM1} < \text{NOTF} < \text{NUM2} < \text{BURY} = 0 < \text{PART}$$

FREE is the initial state of a circle. When a pair of neighboring atoms is first considered, the square of the radius of the intersection circle is calculated (see the section on neighbor relationship). If this radius is small, i.e.,

$$r_{ij}^2 \leq \beta^2 \cdot [\max_i(r_i)]^2$$

(we use $\beta = 0.4$), a check is made if one of the neighboring spheres with the original radius reduced by ε completely contains this intersection circle (sufficiency!). If this NUM1 test is successful, the status of the intersection circle is changed to BURY; otherwise, it is set equal to NUM1. An intersection circle is partly accessible (status PART) if at least one accessible vertex has been located on it.

If a triple i, j, and k is first considered during the search, the triple status products

$$(\text{status}(ij) - B) \cdot (\text{status}(ik) - B) \cdot (\text{status}(jk) - B)$$

with $B \in \{\text{BURY, FREE, NUM1}\}$ are calculated. If the first result is equal to zero and the other two are different from zero, the algorithm proceeds to the next triple. Otherwise, the possible collinearity of the atom triple is checked and h_{ijk}^2 is calculated. In the case of a positive square of the vertex height, the status of all three intersection circles ij, ik, and jk is increased to NOTF. Now, the status product is evaluated again for $B = \text{BURY}$ in the expression above. To this stage, no square roots are necessary.

The coordinates of the base point $\mathbf{b}_{ijk}$ can be calculated with only one square root. The vector product

$$C = [(\mathbf{a}_j - \mathbf{a}_i) \times (\mathbf{a}_k - \mathbf{a}_i)] \times (\mathbf{a}_j - \mathbf{a}_i)$$

is pointing to $\mathbf{b}_{ijk}$ from $\mathbf{t}_{ij}$ if C is multiplied with

$$\sqrt{\frac{r_{ij}^2 - h_{ijk}^2}{|C|^2}} \cdot \text{signum}((\mathbf{a}_j - \mathbf{a}_i) \cdot (\mathbf{t}_{ik} - \mathbf{t}_{ij}))$$

where signum refers to the sign of the expression to follow. For small heights (less than 30% of the maximal sphere radius), we check whether one of the common neighbors of atoms i, j, and k completely contains a sphere with the radius h_{ijk} around $\mathbf{b}_{ijk}$ and, therefore, both possible vertices are buried (base point test).

To obtain the length of the vector pointing from $\mathbf{b}_{ijk}$ to $\mathbf{p}_{ijk}$, a second square root must be extracted:

$$\sqrt{\frac{h_{ijk}^2}{|(\mathbf{a}_j - \mathbf{a}_i) \times (\mathbf{a}_k - \mathbf{a}_i)|^2}}$$

If both vertices above and below the plane ijk have been rejected as buried, then we suppose that the corresponding intersection circles are also completely buried. Here starts the NUM2 test for circles with radii below 70% of the maximal sphere radius. We describe the test for the ij circle. At this stage, the coordinates of a point on the intersection circle are known (the last rejected vertex). The unit vector of $\mathbf{a}_j - \mathbf{a}_i$ is calculated (one square root). A regular polygon with n vertices ($n = 6$) inscribed in the circle ij is constructed with the last rejected vertex as one of the n points (rotating the vertex around the ij unit vector). Also, the n points of a circumscribed regular n-gon are calculated with the vertex as midpoint of one of the edges. As a result, n triangles formed by two successive vertices of the inscribed polygon and one vertex of the outer polygon contain equal and disjunct segments of the circle ij. We check whether these triangles are contained in one of the neighbors. The NUM2 test changes the status of the ij circle to BURY or to NUM2.

Part 3 of the algorithm takes advantage of the orientability of the surface boundary and the definition of incoming and outgoing arcs for vertices. The positive orientation of a surface boundary on the atom i is defined as anticlockwise if viewed ex-

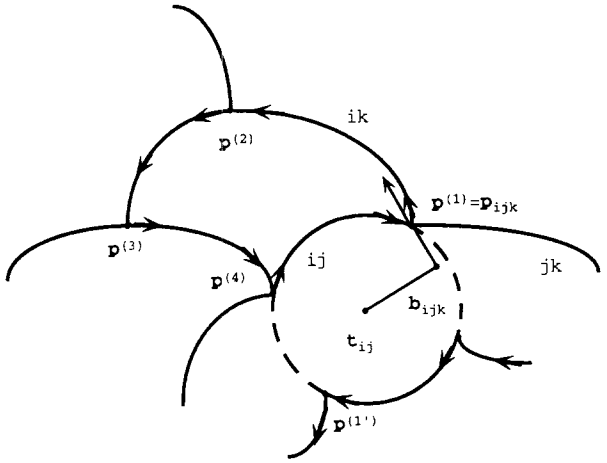

Figure 3. Formation of a cycle. Vertex $\mathbf{p}_{ijk}$ is located on the intersection circles ij (incoming arc) and ik (outgoing arc) of atom i. A cycle is formed by vertices $\mathbf{p}^{(1)}$ ($=\mathbf{p}_{ijk}$), $\mathbf{p}^{(2)}$, $\mathbf{p}^{(3)}$, $\mathbf{p}^{(4)}$, and the respective arcs between them. When searching for succeeding vertices within a cycle and, for example, starting at $\mathbf{p}^{(4)}$, there are two vertices [$\mathbf{p}^{(1)}$ and $\mathbf{p}^{(1')}$] with circle ij as incoming arc from which to choose. An angle criterion [see section (d) of the methods section] is used to select the proper vertex.

ternally from sphere i. Vertex $\mathbf{p}_{ijk}$ on the atom i is located on two circles ij and ik (Fig. 3). Some parts (arcs) of the circles serve as the boundary of the accessible surface of atom i in an environment of $\mathbf{p}_{ijk}$. As a consequence of the boundary orientation, one of the arcs ends in $\mathbf{p}_{ijk}$ (incoming arc) while the other starts in $\mathbf{p}_{ijk}$ (outgoing arc). In the two cases, the angle between the tangent of the incoming arc at the point $\mathbf{p}_{ijk}$ and the vector $\mathbf{p}_{ijk} - \mathbf{b}_{ijk}$ is larger than 90° or less than 90°, respectively. Other situations cannot occur because $h_{ijk} \geq \varepsilon$. Beginning from one vertex $\mathbf{p}^{(1)}$, the next $\mathbf{p}^{(i)}$ ($i = 2, 3, \ldots$) of the cycle has to be searched only among those vertices for which the incoming arc belongs to the same intersection circle as the outgoing arc of the previous vertex $\mathbf{p}^{(i-1)}$ (Fig. 3). The selected vertex minimizes the positively taken angle between the vectors pointing to $\mathbf{p}^{(i-1)}$ and $\mathbf{p}^{(i)}$ from $\mathbf{t}_{ij}$. The positive direction is that of the outgoing arc. This procedure is continued until $\mathbf{p}^{(1)}$ is equal to $\mathbf{p}^{(i)}$ (Fig. 3).

Multiple vertices represent classes of single vertices with only two accessible arcs (Fig. 4). Two conditions using only logical operations may be used for classification. First, all single vertices in a class are located on different atoms. Second, the single vertices in one class can be ordered in such a manner that the outgoing circle of the preceding vertex is the same as the incoming circle of the next vertex. Above all, single vertices in one class must have nearly equal coordinates.

RESULTS AND DISCUSSION

A computer program "ASC" for the *A*nalytic *S*urface *C*omputation of the solvent-accessible surface area

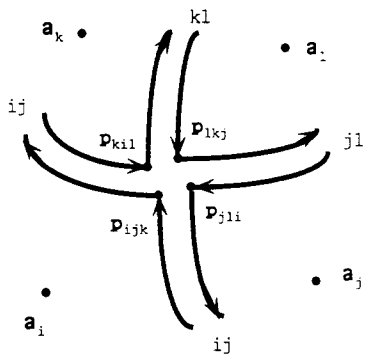

Figure 4. Schematic drawing showing a multiple vertex consisting of four single vertices $\mathbf{p}_{ijk}$, $\mathbf{p}_{jli}$, $\mathbf{p}_{lkj}$, and $\mathbf{p}_{kil}$. The intersection circle that serves as outgoing arc in one vertex is the incoming arc in the next vertex.

as described in the methods section has been written in standard C. A version will be made available; the request should be directed by post or electronic mail to EISENHABER@EMBL-Heidelberg.DE on Internet.

The atomic radii were taken from ref. 12 and r_{sol} was 1.4 Å (1 Å = 10^{-1} nm). We analyzed the behavior of the algorithm for two limits of ε, 10^{-3} Å and 10^{-4} Å. Although the larger value provokes many vertices with unclear arcs, we wished to investigate the stability of the algorithm. The smaller ε value can be considered as a lower limit of ε because $(\varepsilon^2/\text{Å}^2) = 10^{-8}$ is near the accuracy limit of multiple double-precision arithmetics.

To check the program for highly degenerate situations, we used input sets consisting of four and eight spheres on the vertices of a square and a cube, respectively. In the case of the square, the program correctly recognizes eight vertices with only two accessible arcs and four partly accessible circles. In the case of the cube, 24 vertices, each with 2 accessible arcs, and 12 partly accessible intersection circles were found. The same sets were used as input for PQMS. In the first case, the program yielded one of the four spheres as buried and two of them with the same area value, while the fourth had about a 30% lower accessibility. This is an obvious error because the same accessibility should be assigned to all four spheres. Apparently, PQMS recognizes a vertex on the first sphere as buried (because of numerically inaccurate distance calculation) that is located directly on the surface of the other spheres. In the case of the cube, PQMS reported an "INCONSISTENT ROUND-OFF ERROR."

We also calculated the surface of a benzene entity consisting of six carbons at the vertices of a regular hexagon. ASC revealed two multiple vertices, each consisting of six vertices with only two accessible arcs and six partly accessible intersection circles.

Calculation results for a few small- and medium-sized globular proteins are presented in Table I. The rows $n_{que,1}$ and $n_{que,2}$ show the number of vertices

Table I. Data on surface calculation for selected proteins.

	Protein					
	1PPT	4PTI	2PCY	2RHE	3FXN	2UTG
Residues	36	58	99	114	138	140
Atoms	301	454	738	833	1073	1096
A_{ana}	3327.5	3973.8	4966.4	6239.8	6943.8	7198.1
A_{num}	3327.5	3970.9	4954.9	6246.7	6939.9	7192.8
ΔA_{num}	1.3	1.9	1.3	1.5	1.3	1.8
$t_{1,ana}$	0.23	0.64	1.59	1.67	3.21	2.83
	(0.57)	(1.75)	(4.28)	(4.40)	(8.54)	(7.97)
$t_{2,ana}$	2.94	6.23	11.76	12.38	18.11	17.15
	(5.94)	(12.80)	(24.45)	(25.24)	(37.24)	(36.52)
$t_{3,ana}$	3.24	6.73	12.76	13.82	20.31	19.44
	(6.60)	(13.80)	(26.47)	(27.87)	(41.47)	(40.95)
t_{num}	2.41	3.63	6.48	7.03	9.75	9.85
	(4.84)	(8.17)	(15.84)	(16.90)	(23.22)	(23.70)
$n_{que,1}$	17	0	3	7	11	9
$n_{que,2}$	0	0	0	0	2	0
n_{fc}	0	0	0	0	3	1

To illustrate the behavior of ASC, the calculation results for proteins of different sizes are presented. The proteins are named by their respective identification codes in the Brookhaven Protein Data Bank.[32] The proteins are avian pancreatic peptide (1PPT), bovine pancreatic trypsin inhibitor (4PTI), plastocyanin (2PCY), Bence–Jones immunoglobulin (2RHE), flavodoxin (3FXN), and uteroglobulin (2UTG). We used only the ATOM records. A_{ana} is the analytically calculated solvent-accessible surface area in Å^2. We present also the overall surface area A_{num} calculated with a variant of the Shrake–Rupley method[16–19,31] with 377 points per sphere and with distance class formation for atoms and points. ΔA_{num} is the maximal deviation from the analytic results in the atom-by-atom comparison. The processing time consumption of the analytic algorithm was measured at three stages: after the neighbor list calculation t_{num} ($t_{1,ana}$), after the determination of the list of accessible vertices and intersection circles ($t_{2,ana}$), and after the area calculation ($t_{3,ana}$). The time values are given in seconds with the first listed number resulting from computation on one R3000 processor of an SGI 4D/480 (5–6 MFLOP), and the second number below in parentheses corresponds to the DEC station 5000/125 (about 2.5 MFLOP). The value t_{num} is the CPU time for the numerical surface calculation with the 377-point Shrake and Rupley method. The rows $n_{que,1}$ and $n_{que,2}$ list the number of vertices with unclear arcs for $\varepsilon = 10^{-3}$ Å and $\varepsilon = 10^{-4}$ Å, respectively. The value n_{fc} represents the number of free intersection circles.

with unclear arcs encountered during the formation of the list of accessible vertices and intersection circles in the two cases $\varepsilon = 10^{-3}$ Å and $\varepsilon = 10^{-4}$ Å, respectively. The area results do not differ in both cases but the surface topology may vary somewhat. For example, no differences were observed for 1 PPT. The algorithm had the choice between three four-membered multiple vertices and three pairs of classical vertices connected with a short arc for the larger ε. In correspondence with the selection criteria, the algorithm suppresses multiple vertices and selected the only variant obtained with the smaller ε. In the case of the larger ε, the algorithm can offer more variants for topological closure of the surface. However, it does reject possibilities with arcs smaller than ε, which may be allowed with application of a decreased ε. As a result, the surface of 2RHE is closed for the larger ε only if a four-membered multiple vertex is admitted (atoms 488-LYS67, 496-SER68, 515-SER71, and 520-ALA72). Another multiple vertex is formed by atoms 601-GLY79 and atoms 603, 604, and 608 of LYS80 on the accessible surface of 3FXN. For $\varepsilon = 10^{-4}$ Å, two classical vertices with a connecting arc shorter than 10^{-3} Å replace the multiple vertex. Vertices with unclear arcs do occur also in the case $\varepsilon = 10^{-4}$ Å (e.g., 3FXN) but the ambiguity can be removed by application of the topological closure criterion.

Regarding the accuracy differences between the present analytic technique and commonly used numerical methods, we present the overall surface area A_{num} calculated with a variant of the Shrake–Rupley method[16–19,31] with 377 points per sphere (Table I). Although the summed area values do not differ much, the absolute error for particular atoms is large (up to 1.9 Å^2). This effect is important if the energy weight per Å^2 is large such as in the parameter set of Ooi et al.[33] (0.43 kcal/mol for carbonyl and carboxyl carbons).

The computational performance of the analytic algorithm is boosted by our improvements (see Table I). The times given in Table I relate to that required for each of the three major tasks: $t_{1,ana}$ for determination of the neighbor list; ($t_{2,ana} - t_{1,ana}$, the largest part of $t_{3,ana}$) to effect the list of accessible intersection circles and vertices; ($t_{3,ana} - t_{2,ana}$) to calculate the area. $t_{3,ana}$ as the overall time is already in the range of fast numerical routines (t_{num}). Only the effect of the NUM1, NUM2, and the base point tests reduces the CPU time by a factor of 4–5 for compact structures. For the example of 3FXN, the NUM1 test is activated for 5107 intersection circles.

In 4496 cases, the circle was recognized as buried. The NUM2 test was successful for 7160 of 8599 intersection circles. The total number of intersection circles for 3FXN is 23,669. As a result, both tests together recognized about 50% of them as buried. The base point test was successful in 1268 of 1780 cases. Collinear atom triples are, as a rule, accompanied by one small intersection circle. This circle is mostly already removed from consideration by the NUM1 test. Therefore, the frequency of encountering collinear triples became small.

The application of the modifications described in this article require negligible processing time. We could not observe a dependency of the CPU time in the range of ε studied. The processing time depends strongly on the mean number of neighbors per atom because of the evaluation of the status of more intersection circles. One surface calculation for a conformation of crambin with the current version of the program takes between 1.50 and 4.29 s of CPU time on one processor of the SGI 4D 480 machine (5–6 MFLOP) depending on the compactness of the conformation where the limits correspond to a fully extended or a fully folded chain (Table II). Coordinates of the regularized conformations of crambin were obtained with ICM.[31,34–37] Surprisingly, more processing time is necessary for 3FXN than for 2UTG, although 2UTG has more heavy atoms, i.e., 3FXN is very compact.

Table II. Influence of conformation on the surface area calculation.

	Protein		
	1CRN	$CRN_{compact}$	$CRN_{extended}$
A_{ana}	2988.3	2974.2	5813.5
A_{num}	2984.9	2975.7	5819.5
ΔA_{num}	1.1	1.9	1.7
$t_{1,ana}$	0.41	0.40	0.09
	(0.95)	(0.99)	(0.17)
$t_{2,ana}$	3.99	3.98	1.00
	(8.17)	(8.09)	(1.77)
$t_{3,ana}$	4.27	4.29	1.50
	(8.77)	(8.64)	(2.62)
t_{num}	2.70	2.58	1.60
	(5.71)	(5.75)	(3.42)
$n_{quc,1}$	3	0	6
$n_{quc,2}$	0	0	0

The data shows the dependency of computation efficiency on structural compactness. Crambin is a protein consisting of 46 residues and 327 heavy atoms. The data is presented for the PDB version (1CRN), for a regularized near-crystal structure ($CRN_{compact}$), and for a fully extended conformation ($CRN_{extended}$). The rows are assigned as in Table I. The atom coordinates for the regularized conformations of crambin were obtained with the program package ICM.[31,34–37] In the case of the extended structure, the analytic routine is faster than the numerical 377-point Shrake and Rupley method (see legend of Table I). The analytic routine's processing time is increased by a factor of about 3 for compact crambin. The folding of crambin reduces the accessible surface by 50%.

For crambin, the CPU time of Richmonds program[23] executed on a MicroVAX II is 260.18 s.[5] The nonvectorized version of MSEED[26] takes 0.51 s for crambin and 0.71 s for the bovine pancreatic trypsin inhibitor (BPTI) in the single-processor mode on an IBM 3090/600J (16 MFLOP). ANA, a program designed by Connolly, needs 8.27 s for crambin and 12.13 s for BPTI.[26] Taking the performance differences between their and our computers into account, our implementation ASC is only two to three times slower than MSEED and six to nine times faster than ANA (cf. Table I in ref. 26).

It is of importance to design the analytic surface algorithm in such a way that, in addition to the inherent singular cases, no other undefined situations occur from the mathematical formulation itself. In the approach of Richmond,[23] a matrix **T** is calculated [eqs. (14)–(19)] for rotating the $\mathbf{v}_{ij} = (\mathbf{a}_i - \mathbf{a}_j)/d_{ij}$ onto the z-axis of the atomic coordinate system. If the angle between the two vectors gives a sine near zero, **T** is not defined. **T** may be set equal to the unit matrix, but derivatives of **T** with respect to atom coordinates are indeterminable at this singularity.

Our results also demonstrate that one cannot rely on the possible absence of free circles for the accessible surface of globular proteins as proposed in ref. 26. A few examples have been observed in 3FXN and 2UTG (Table I).

CONCLUSIONS

The modified analytic algorithm for surface area calculations allows singular and degenerate cases to be handled correctly and avoids large (topological) errors in the surface determination. These considerations are especially important if a series of conformations are to be evaluated such as those encountered in Monte Carlo simulations or if surface derivatives with respect to Cartesian[23,26] or internal[27] coordinates are to be computed for energy minimizations. The efficiency improvements of the algorithm discussed here together with other modifications to speed the calculations should pave the way for broader application of analytically calculated surface energy terms in molecular mechanics.[6,23,26,38,39]

F.E. is grateful to Ruben Abagyan for generously giving insight into details of his program package ICM. F.E. also thanks Philip Lijnzaad for tutorials in using UNIX and C and is grateful to Maxim Totrov for helpful discussions. The authors are grateful to K.-H. Gross for introduction to the program PQMS. They are also thankful for financial support (Grant FG5-1075 to P.A.) from the German Bundesministerium für Forschung und Technologie.

References

1. W. Kauzmann, *Adv. Prot. Chem.*, **14,** 1 (1959).
2. C. Tanford, *The Hydrophobic Effect*, 2nd ed., Wiley Interscience, New York, 1980.

3. J. Novotny, R. Bruccoleri, and M. Karplus, *J. Mol. Biol.*, **177,** 787 (1984).
4. G. Baumann, C. Frömmel, and C. Sander, *Prot. Eng.*, **2,** 329 (1989).
5. W. Hasel, T. Hendrickson, and W.C. Still, *Tetr. Comp. Meth.*, **1,** 103 (1988).
6. W.C. Still, A. Tempczyk, R.C. Hawley, and T. Hendrickson, *J. Am. Chem. Soc.*, **112,** 6127 (1990).
7. I. Langmuir, *Third Colloid Symposium Monograph*, Chemical Catalog Co., New York, 1925, pp. 48–75.
8. K.A. Sharp, A. Nicholls, R.F. Fine, and B. Honig, *Science*, **252,** 106 (1990).
9. K.A. Sharp, A. Nicholls, R. Friedman, and B. Honig, *Biochemistry*, **30,** 9686 (1991).
10. E. Silla, I. Tunon, and J.L. Pascual-Ahuir, *J. Comp. Chem.*, **12,** 1077 (1991).
11. I. Tunon, E. Silla, and J.L. Pascual-Ahuir, *Prot. Eng.*, **5,** 715 (1992).
12. D. Eisenberg and A.D. McLachlan, *Nature*, **319,** 199 (1986).
13. J. Vila, R.L. Williams, M. Vasquez, and H.A. Scheraga, *Proteins*, **10,** 199 (1991).
14. B. Lee and F.M. Richards, *J. Mol. Biol.*, **55,** 379 (1971).
15. F.M. Richards, *Annu. Rev. Biophys. Bioeng.*, **6,** 151 (1977).
16. A. Shrake and J.A. Rupley, *J. Mol. Biol.*, **79,** 351 (1973).
17. J.L. Pascual-Ahuir and E. Silla, *J. Comp. Chem.*, **12,** 1047 (1991).
18. H. Wang and C. Levinthal, *J. Comp. Chem.*, **12,** 868 (1991).
19. S.M. LeGrand and K.M.M. Merz Jr., *J. Comp. Chem.*, **14,** 349 (1993).
20. M.Y. Pavlov and B.A. Fedorov, *Biopolymers*, **22,** 1507 (1983).
21. M.L. Connolly, *J. Appl. Cryst.*, **16,** 548 (1983).
22. M.L. Connolly, *J. Appl. Cryst.*, **18,** 499 (1985).
23. T.J. Richmond, *J. Mol. Biol.*, **178,** 63 (1984).
24. K.D. Gibson and H.A. Scheraga, *Mol. Phys.*, **62,** 1247 (1987).
25. K.D. Gibson and H.A. Scheraga, *Mol. Phys.*, **64,** 641 (1988).
26. G. Perrot, B. Cheng, K.D. Gibson, J. Vila, K.A. Palmer, A. Nayeem, B. Maigret, and H.S. Scheraga, *J. Comp. Chem.*, **13,** 1 (1992).
27. F. Eisenhaber and P. Argos, to be published.
28. M. Connolly, *Molecular Surface Package pqms, srf and trb, Implementation Manual and User's Manual*, 1991.
29. M.P. do Carmo, *Differential Geometry of Curves and Surfaces*, Prentice-Hall, NJ, Englewood Cliffs, 1976, pp. 264–283.
30. D.B. Beglov and A.A. Lipanov, *J. Biomol. Struct. Dyn.*, **9,** 205 (1991).
31. R.A. Abagyan and M.M. Totrov, personal communication.
32. F.C. Bernstein, T.F. Koetzle, G.J.B. Williams, E.F. Meyer Jr., M.D. Brice, J.R. Rodgers, O. Kennard, T. Shimanouchi, and M. Tasumi, *J. Mol. Biol.*, **112,** 535 (1977).
33. T. Ooi, M. Ootobake, G. Nemethy, and H.A. Sceraga, *Proc. Natl. Acad. Sci. USA*, **84,** 3086 (1977).
34. A.K. Mazur and R.A. Abagyan, *J. Biomol. Struct. Dyn.*, **6,** 815 (1989).
35. R.A. Abagyan and A.K. Mazur, *J. Biomol. Struct. Dyn.*, **6,** 833 (1989).
36. R.A. Abagyan and P. Argos, *J. Mol. Biol.*, **225,** 519 (1992).
37. R.A. Abagyan, M.M. Totrov, and D.A. Kuznetsov, personal communication.
38. L. Wesson and D. Eisenberg, *Prot. Sci.*, **1,** 227 (1992).
39. C.A. Schiffer, J.W. Caldwell, R.M. Stroud, and P.A. Kollman, *Prot. Sci.*, **1,** 396 (1992).